

**MEASUREMENT OF  $D_s^* - D_s$  MASS DIFFERENCE**

ARGUS Collaboration

H. ALBRECHT, U. BINDER <sup>1</sup>, P. BÖCKMANN, R. GLÄSER, G. HARDER, A. KRÜGER, A. NIPPE,  
M. SCHÄFER, W. SCHMIDT-PARZEFALL, H. SCHRÖDER, H.D. SCHULZ, F. SEFKOW,  
R. WURTH, A. YAGIL <sup>2,3</sup>

*DESY, D-2000 Hamburg 52, Fed. Rep. Germany*

R.D. APPUHN, J.P. DONKER, A. DRESCHER, D. KAMP, H. KOLANOSKI, U. MATTHIESEN,  
H. SCHECK, G. SCHWEDA, B. SPAAN, J. SPENGLER, A. WALTHER, D. WEGENER

*Institut für Physik, Universität Dortmund <sup>4</sup>, D-4600 Dortmund, Fed. Rep. Germany*

J.C. GABRIEL, T. RUF, K.R. SCHUBERT, J. STIEWE, K. STRAHL, R. WALDI, S. WERNER

*Institut für Hochenergiephysik, Universität Heidelberg <sup>5</sup>, D-6900 Heidelberg, Fed. Rep. Germany*

K.W. EDWARDS <sup>6</sup>, W.R. FRISKEN <sup>7</sup>, D.J. GILKINSON <sup>8</sup>, D.M. GINGRICH <sup>8</sup>, H. KAPITZA <sup>6</sup>,  
P.C.H. KIM <sup>8</sup>, R. KUTSCHKE <sup>8</sup>, D.B. MACFARLANE <sup>9</sup>, J.A. McKENNA <sup>8</sup>, K.W. McLEAN <sup>9</sup>,  
A.W. NILSSON <sup>9</sup>, R.S. ORR <sup>8</sup>, P. PADLEY <sup>8</sup>, J.A. PARSONS <sup>8</sup>, P.M. PATEL <sup>9</sup>, J.D. PRENTICE <sup>8</sup>,  
H.C.J. SEYWERD <sup>8</sup>, J.D. SWAIN <sup>8</sup>, G. TSIPOLITIS <sup>9</sup>, T.-S. YOON <sup>8</sup>, J.C. YUN <sup>6</sup>

*Institute of Particle Physics <sup>10</sup>, Canada*

R. AMMAR, S. BALL, D. COPPAGE, R. DAVIS, S. KANEKAL, N. KWAK

*University of Kansas <sup>11</sup>, Lawrence, KS 66045, USA*

B. BOŠTJANČIČ, G. KERNEL, P. KRIŽAN, M. PLEŠKO

*Institut J. Stefan and Oddelek za fiziko, Univerza v Ljubljana <sup>12</sup>, 61111 Ljubljana, Yugoslavia*

L. JÖNSSON

*Institute of Physics, University of Lund <sup>13</sup>, S-223 62 Lund, Sweden*

A. BABAIEV, M. DANILOV, B. FOMINYKH, A. GOLUTVIN, I. GORELOV, V. LUBIMOV,  
V. MATVEEV, V. RYLTSOV, A. SEMENOV, V. SHEVCHENKO, V. SOLOSHENKO,  
V. TCHISTILIN, I. TICHOMIROV, Yu. ZAITSEV

*Institute of Theoretical and Experimental Physics, 117 259 Moscow, USSR*

R. CHILDERS, C.W. DARDEN, R.C. FERNHOLZ, Y. OKU

*University of South Carolina <sup>14</sup>, Columbia, SC 29208, USA*

Received 3 December 1987

Using the ARGUS detector at DORIS, we observe the production of  $D_s^{*+}$  mesons in  $e^+e^-$  annihilation through their subsequent decays to a  $D_s^+$  and a photon. Photons which convert in the beam pipe or drift chamber inner wall are used to obtain a high precision measurement of the  $D_s^{*+}-D_s^+$  mass difference, while photons detected in the shower counters are used to determine the production cross section, and to provide an independent measurement of the  $D_s^{*+}-D_s^+$  mass difference. The observed  $D_s^{*+}-D_s^+$  mass difference is  $142.5 \pm 0.8 \pm 1.5$  MeV/ $c^2$ , and  $\sigma(e^+e^- \rightarrow D_s^{*+} X) \cdot \text{BR}(D_s^{*+} \rightarrow D_s^+ \gamma) (\cdot \text{BR}(D_s^+ \rightarrow \phi \pi^+))$  is  $4.4 \pm 1.1 \pm 1.0$  pb at 10.2 GeV. The width of the  $D_s^{*+}$  is less than 4.5 MeV/ $c^2$  at 90% confidence level.

The  $D_s^{*+}$  meson <sup>#1</sup>,  $J^P=1^-, I=0$  (formerly known as  $F^{*+}$ ) predicted by the quark model [1], has been observed by a number of experiments, including ARGUS [2], TPC [3], and, more recently, MARK III [4]. Isospin conservation forbids the strong decay to  $D_s^+ \pi^0$ , leaving the electromagnetic decay  $D_s^{*+} \rightarrow D_s^+ \gamma$  as the dominant mode. Hitherto the  $D_s^{*+}-D_s^+$  mass difference has been measured with an accuracy of order 10 MeV/ $c^2$ . In order to confront the theoretical calculations [5], a much higher precision is necessary. In this letter we report on the results of such a high precision measurement, the combined statistical and systematic uncertainty being reduced to 2 MeV/ $c^2$ . The analysis uses only the  $D_s^+ \rightarrow \phi \pi^+$  decay channel of the  $D_s^+$ , in order to obtain a  $D_s^+$  signal with low background.

The data presented here were collected using the ARGUS detector at the DORIS II  $e^+e^-$  storage ring at DESY. The centre-of-mass energy covered a range from 9.4 to 10.6 GeV, with a weighted mean of 10.2

GeV. Data used in this analysis are derived from a 255.5 pb<sup>-1</sup> sample, comprising 45.0 pb<sup>-1</sup> on  $\Upsilon(1S)$ , 36.8 pb<sup>-1</sup> on  $\Upsilon(2S)$ , 103.1 pb<sup>-1</sup> on  $\Upsilon(4S)$  and 70.5 pb<sup>-1</sup> in the continuum and resonance scanning. This corresponds to approximately two million multihadron events. A brief description of the detector, trigger, and multihadron selection criteria may be found in ref. [6].

For charged particle identification, the specific ionization ( $dE/dx$ ) in the drift chamber, the time-of-flight (TOF), muon counter and shower counter information are used to form an overall  $\chi^2$  for each particle species hypothesis. The likelihood for each particle hypothesis is determined for every charged track in an event; details of the procedure may be found in ref. [7]. Most tracks with momentum below 800 MeV/ $c$  are uniquely identified, thus reducing combinatorial background.

All  $K^+K^-$  combinations which have a  $\chi^2$  of less than 16 for the  $\phi$  mass hypothesis, and which fall within 12 MeV/ $c^2$  of the nominal  $\phi$  mass, are considered as  $\phi$  candidates. Subsequently,  $D_s^+$  candidates are formed by adding a  $\pi^+$  to the  $\phi$  candidates. Since the  $D_s^+$  has zero spin, the angular distribution of its decay products in its rest frame is uniform. A major background to the  $D_s^+$  signal arises from combinations of  $\phi$ 's with unassociated pions [8]. The angular distribution,  $\cos \theta_\phi$ , of the  $\phi$  with respect to the  $D_s^+$  in the  $D_s^+$  rest frame, of this background is peaked towards  $\cos \theta_\phi = 1$ ; the signal, however, is uniformly distributed. By selecting  $\phi \pi$  combinations where  $\cos \theta_\phi < 0.8$ , almost half of this background is eliminated, while retaining 90% of the signal. Similarly, since the  $\phi$  has spin one, conservation of angular momentum requires that the  $\phi$  and the  $\pi$  be in an  $l=1$  state, and that the  $\phi$  has zero helicity in the  $D_s^+$  rest frame. This results in  $K$  mesons from the  $D_s^+$  signal having a  $\cos^2 \theta_{K^+}$  distribution, where  $\theta_{K^+}$  is the angle

<sup>1</sup> Present address: CERN, CH-1211 Geneva 23, Switzerland.

<sup>2</sup> Weizmann Institute of Science, 76100 Rehovot, Israel.

<sup>3</sup> Supported by the Minerva Stiftung.

<sup>4</sup> Supported by the German Bundesministerium für Forschung und Technologie, under the contract number 054DO51P.

<sup>5</sup> Supported by the German Bundesministerium für Forschung und Technologie, under the contract number 054HD24P.

<sup>6</sup> Carleton University, Ottawa, Ontario, Canada K1S 5B6.

<sup>7</sup> York University, Downview, Ontario, Canada M3J 1P3.

<sup>8</sup> University of Toronto, Toronto, Ontario, Canada, M5S 1A7.

<sup>9</sup> McGill University, Montreal, Quebec, Canada H3A 2T8.

<sup>10</sup> Supported by the Natural Sciences and Engineering Research Council, Canada.

<sup>11</sup> Supported by the US National Science Foundation.

<sup>12</sup> Supported by Raziskovalna skupnost Slovenije, the Internationales Büro KfA, Jülich, and DESY, Hamburg.

<sup>13</sup> Supported by the Swedish Research Council.

<sup>14</sup> Supported by the US Department of Energy, under contract DE-AS09-80ER 10690.

<sup>#1</sup> References in this paper to a specific charged state are to be interpreted as implying the charge conjugate state also.

of the  $K^+$  with respect to the  $\pi^+$ , in the  $\phi$  rest frame. Uncorrelated background results in a uniform distribution in  $\cos \theta_{K^+}$ ; 50% of the background, and only 12.5% of the signal are removed by requiring that  $|\cos \theta_{K^+}| > 0.5$ . These two angular cuts are used in the  $D_s^*$  analysis. In fig. 1, we invoke the fact that  $D_s^*$  mesons are produced with high momentum due to the hard fragmentation function associated with primary charmed meson production [9], and require that the reduced momentum of the  $D_s^*$ ,  $x_p = p_{D_s^*}/p_{max}$ , be greater than 0.5.

The  $\phi\pi^+$  invariant mass spectrum obtained after the two angular cuts, plus the cut on reduced momentum, is shown in fig. 1. There is a clear enhancement at a mass of  $1968.8 \pm 1.4 \pm 3.0 \text{ MeV}/c^2$ , with an RMS width of  $13.8 \pm 1.3 \text{ MeV}/c^2$ . The width is consistent with that expected from the experimental resolution. A smaller enhancement at a mass near  $1870 \text{ MeV}/c^2$  corresponds to the Cabibbo suppressed decay of the  $D^+$  meson, seen in the  $D^+ \rightarrow \phi\pi^+$  decay mode. The  $\sigma(e^+e^- \rightarrow D_s^* X) \cdot \text{BR}(D_s^* \rightarrow \phi\pi^+)$  is  $7.8 \pm 0.8 \pm 1.3 \text{ pb}$  at  $10.2 \text{ GeV}$ , extrapolated over the entire  $x_p$  range [7].

To obtain our best result for the mass of the  $D_s^*$ , we consider the mass of the  $D^0$  to be  $1864.1 \pm 1.4 \text{ MeV}/c^2$ , as measured by ARGUS [10], which is  $0.5 \text{ MeV}/c^2$  lower than the world average [11]. Correcting the  $D_s^*$  mass by this systematic shift yields a mass measurement of  $1969.3 \pm 1.4 \pm 1.4 \text{ MeV}/c^2$ .

To search for a  $D_s^{*+}$  signal we have combined photons with all  $\phi\pi^+$  combinations within  $20 \text{ MeV}/c^2$  of

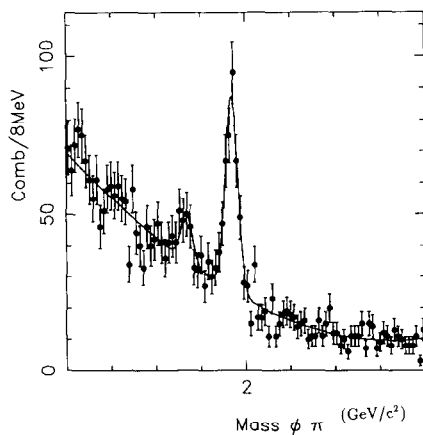


Fig. 1.  $\phi\pi^+$  mass spectrum, with  $x_p > 0.5$ , and angular cuts  $\cos \theta_c < 0.8$ , and  $|\cos \theta_K| > 0.5$ .

the  $D_s^*$  mass, and which have a  $\chi^2$  for the  $D_s^*$  mass hypothesis of less than 16.

The photons are detected by two very different methods. Firstly, photon energies are measured using the array of shower counters. These showering photons we denote by  $\gamma_s$ ; they are measured with high efficiency in the energy range used in this analysis, and an energy resolution of approximately 12% at  $0.5 \text{ GeV}$  [12]. Fig. 2a shows the  $\gamma_s\gamma_s$  invariant mass distribution. The  $\pi^0$  is clearly seen at a mass of

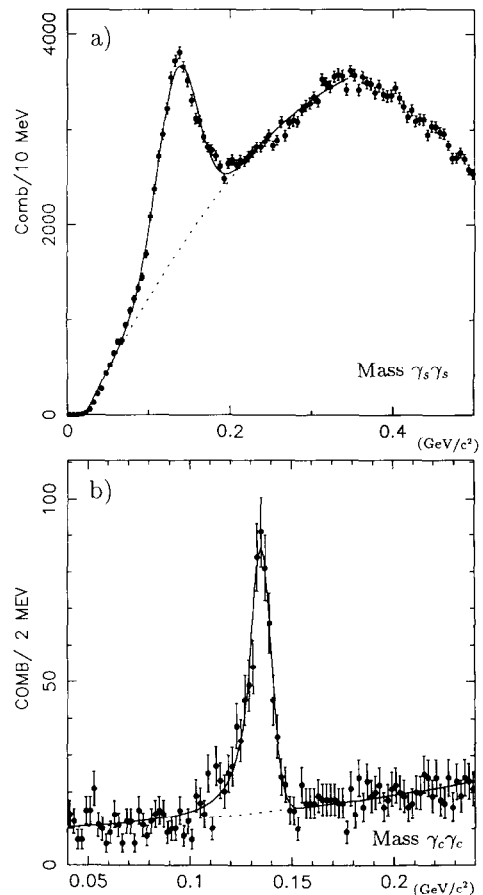


Fig. 2. (a) Mass spectrum  $\gamma_s\gamma_s$ , showing the neutral pion decaying to two showering photons. The photons are in the energy range of interest in decays of continuum produced  $D_s^{*+}$ ,  $E_\gamma > 0.15 \text{ GeV}$ . The distribution is fitted with a gaussian, plus a radiative tail. (b) Mass spectrum  $\gamma_c\gamma_c$ , showing neutral pion decaying to two converting photons. The photons are in the energy range relevant in decays of  $D_s^{*+}$ , with good reconstruction efficiency,  $0.1 < E_\gamma < 0.6 \text{ GeV}$ .

$135.3 \pm 0.3 \pm 4.0 \text{ MeV}/c^2$ , with a width of  $23.4 \pm 0.4 \text{ MeV}/c^2$ . This gives confidence in both the overall calibration of the shower counter system and also the resolution. The high efficiency of this method of photon detection allows us to perform a statistically significant measurement of the production cross section of the  $D_s^{*+}$  multiplied by the branching ratio to the  $\phi\pi^+$  final state of the  $D_s^+$ .

The resolution of the  $D_s^{*+} - D_s^+$  mass difference is dramatically improved by using the second method of photon detection. This method exploits the fact that there is about a 3% probability of photons converting to  $e^+e^-$  pairs in the beam pipe, or inner wall of the main drift chamber; these converting photons we denote by  $\gamma_c$ . The resolution with which the energy of these photons is measured is governed by the precise momentum resolution of the ARGUS drift chamber:

$$\sigma_p/p = \sqrt{(0.014p)^2 + (0.01)^2}, \quad (1)$$

where  $p$  is in  $\text{GeV}/c$ . The reconstruction of the  $\gamma_c$  proceeds by finding a secondary vertex formed by an  $e^+e^-$  pair. Requiring the invariant mass of each conversion pair to be less than  $10 \text{ MeV}/c^2$  results in the  $\gamma_c\gamma_c$  invariant mass distribution shown in fig. 2b. The  $\pi^0$  signal is fitted with a gaussian plus radiative tail. The resulting mass and RMS width are  $134.8 \pm 0.4 \pm 1.0 \text{ MeV}/c^2$  and  $5.2 \pm 0.4 \text{ MeV}/c^2$ , a considerable improvement on the  $\pi^0$  signal obtained using the  $\gamma_s$ .

Using the first method of photon detection, the  $D_s^+$  candidates are combined with shower counter photons. There is a large background from low energy uncorrelated photons. This results in a given  $D_s^+$  candidate combining with several photons to produce more than one  $D_s^{*+}$  candidate in the 130–150  $\text{MeV}/c^2$  mass difference region. This double counting effect is rendered negligible, and the general background is substantially reduced, by requiring that the photons have an energy greater than 180 MeV. Since one expects the  $D_s^{*+}$  production to be from primary continuum charm particle production, we exploit the hard charm fragmentation by requiring that  $x_p > 0.5$  for the  $D_s^+\gamma_s$  system. The data sample used includes data from the  $\Upsilon(4S)$ , and clearly there could be  $D_s^{*+}$  production from the decay of B mesons. The  $x_p$  cut selects combinations beyond the kinematic limit for  $D_s^{*+}$  from B decay, ensuring that only events

from continuum production are included. The mass difference spectrum,  $\Delta M = m(D_s^+\gamma_s) - m(D_s^+)$ , is shown in fig. 3a. A significant peak is seen at  $\Delta M$  near  $140 \text{ MeV}/c^2$ , rather close to the threshold in the mass difference distribution. The shape of the background dominates the systematic error on the measured mass difference. It has been determined in two ways. Firstly, by Monte Carlo; secondly, by fitting to the shape of the mass difference distribution resulting when the  $\phi\pi^+$  combinations are required to lie outside of the  $D_s^+$  region. This latter distribution is shown in fig. 3b. These two determinations of the background shape give consistent results. In fitting the distributions in figs. 3a and 3b, the background shape is determined using Monte Carlo; it is a third order polynomial with a threshold factor. The signal is fitted with a gaussian with width fixed to the value

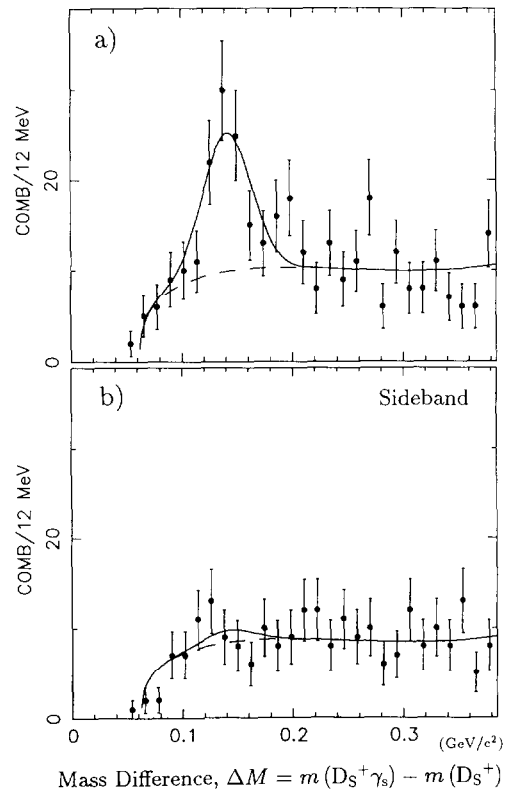


Fig. 3. (a) Mass difference spectrum using showering photons,  $\Delta M = m(D_s^+\gamma_s) - m(D_s^+)$ . (b) Mass difference spectrum, with the  $\phi\pi$  taken from the  $D_s$  sideband, within  $50 \text{ MeV}/c^2$  of  $m(\phi\pi) = 2.16 \text{ GeV}/c^2$ .

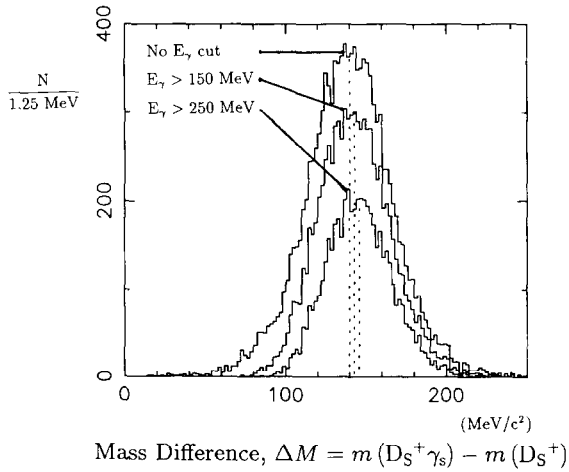


Fig. 4. Shift of  $\Delta M$  peak as a function of photon energy cut.

$21.7 \text{ MeV}/c^2$ , as determined by the Monte Carlo. The fit results in  $68.8^{+13.0}_{-12.3}$  events in the signal, and an uncorrected mass difference of

$$\Delta M = m(D_S^+ \gamma_s) - m(D_S^+) = 141.7 \pm 4.8 \text{ MeV}/c^2. \quad (2)$$

Fitting the same background and signal shape to the sideband distribution in fig. 3b does not result in a statistically significant signal:  $6.1^{+9.3}_{-8.6}$  events at a mass difference of  $141.7 \text{ MeV}/c^2$ . Due to the finite resolution of the photon energy measurement, the requirement that the photons have an energy greater than  $180 \text{ MeV}$  introduces an experimental bias to larger mass differences. In fig. 4 we show the result of a Monte Carlo simulation of this bias; as the photon energy cut increases, the  $D_S^{*+} - D_S^+$  mass difference effectively shifts to higher values. In this way we estimate that the cuts applied to the data yield a mass difference shift of  $3.1 \text{ MeV}/c^2$ , resulting in a corrected value of  $\Delta M = 138.6 \pm 4.8 \pm 4.0 \text{ MeV}/c^2$ . The corrected result is listed in table 1. In extracting the production cross section multiplied by the branching

Table 1

	Mass ( $\text{MeV}/c^2$ )	Width ( $\text{MeV}/c^2$ )	Number events
$D_S^+ \gamma_s$	$138.6 \pm 4.8 \pm 4.0$	21.7	$68.8^{+13.0}_{-12.3}$
$D_S^+ \gamma_c$	$142.9 \pm 0.8 \pm 1.6$	2.0	$9.9^{+3.8}_{-3.0}$
combined	$142.5 \pm 0.8 \pm 1.5$		

ratio of the  $D_S^{*+}$  to  $\phi\pi^+$  we must correct for the effect of the cut on  $x_p$ , the reduced momentum. This is done by extrapolating over all  $x_p$ , using the Peterson et al. fragmentation function [9] with parameter [7]  $\epsilon = 0.04^{+0.03}_{-0.01}$ , which results in  $\sigma(e^+e^- \rightarrow D_S^{*+} X) \cdot \text{BR}(D_S^{*+} \rightarrow D_S^+ \gamma) \cdot \text{BR}(D_S^+ \rightarrow \phi\pi^+) = 4.4 \pm 1.1 \pm 1.0 \text{ pb}$  for the production of  $D_S^{*+}$  from the continuum. The systematic error is dominated by the extrapolation of the fragmentation function. We deduce that  $(56 \pm 22 \pm 11)\%$  of  $D_S^+$  are produced from  $D_S^{*+}$ .

In using the converted photons to make a precise measurement of the mass difference, we have relaxed some of the kinematical cuts mentioned above, in order to increase the acceptance. The relaxed cuts are  $\cos\theta_\phi < 0.9$  and a mass cut around the  $D_S^+$  of  $\pm 25 \text{ MeV}/c^2$ . The cut of  $|\cos\theta_{K^+}| > 0.5$  is unchanged. Converted photons are combined with  $D_S^+$  candidates; the resulting mass difference spectrum,  $\Delta M = m(D_S^+ \gamma_c) - m(D_S^+)$ , is shown in fig. 5a. The narrow peak at a mass difference near  $140 \text{ MeV}/c^2$  is fitted with a gaussian of fixed width  $2.0 \text{ MeV}/c^2$ , allowing for the radiative tail, while the background is

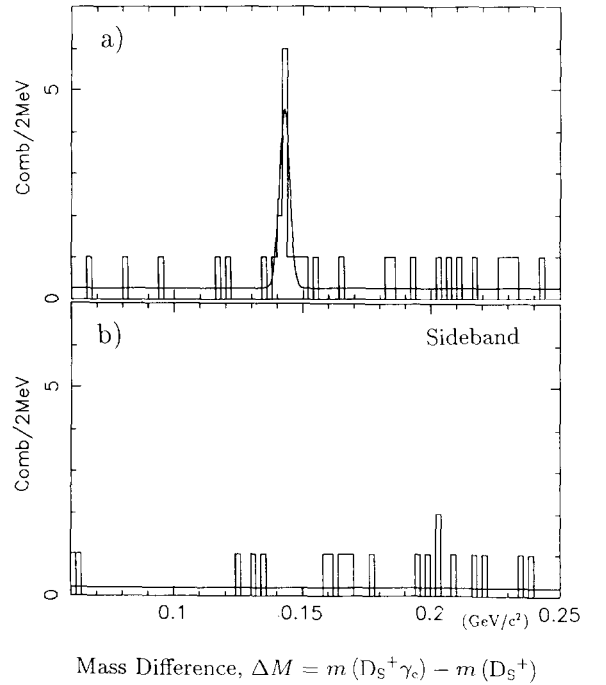


Fig. 5. (a) Mass difference spectrum using converted photons,  $\Delta M = m(D_S^+ \gamma_c) - m(D_S^+)$ . (b) Mass difference spectrum, with  $\phi\pi$  taken from sideband, within  $25 \text{ MeV}/c^2$  of  $m(\phi\pi) = 2.15 \text{ GeV}/c^2$ .

flat. Fitting to this distribution results in a signal of  $9.9_{-3.0}^{+3.7}$  events, at a mass difference of

$$\Delta M = m(D_s^+ \gamma_c) - m(D_s^+) = 142.9 \pm 0.8 \text{ MeV}/c^2. \quad (3)$$

Allowing the width of the signal to vary yields  $\Gamma(D_s^{*+}) < 4.5 \text{ MeV}/c^2$  at 90% CL. No signal is evident when the  $D_s^+$  is taken from the sideband region, as seen in fig. 5b.

We verify the mass scale by using the measured value of the  $D^{*0}-D^0$  mass difference. We have measured this mass difference using the process,

$$D^{*0} \rightarrow D^0 \gamma_c \quad (4)$$

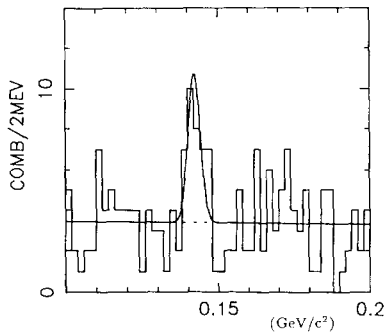
where  $D^0 \rightarrow K^- \pi^+$ ,  $D^0 \rightarrow K^- \pi^+ \pi^+ \pi^-$ ,

which has very similar systematics to the process under study, although it has a much larger background, due to the many photons correlated with  $D^0$  mesons, through the decay  $D^{*0} \rightarrow D^0 \pi^0$ . The mass difference spectrum  $\Delta M = m(D^0 \gamma_c) - m(D^0)$ , is shown in fig. 6. The  $D^{*0}-D^0$  mass difference is  $142.2 \pm 0.9 \text{ MeV}/c^2$ , in good agreement with the Particle Data Group value [11] of  $142.5 \pm 1.3 \text{ MeV}/c^2$ . The quoted systematic error on the  $D_s^{*+}-D_s^+$  mass difference is dominated by the Particle Data Group's statistical error on the  $D^{*0}-D^0$  mass difference.

In conclusion, the production cross section from continuum at  $\langle E_{CM} \rangle = 10.2 \text{ GeV}$  is

$$\sigma(D_s^{*+}) \cdot \text{BR}(D_s^{*+} \rightarrow D_s^+ \gamma) \cdot \text{BR}(D_s^+ \rightarrow \phi \pi^+) = 4.4 \pm 1.1 \pm 1.0 \text{ pb} \quad (5)$$

or



Mass Difference,  $\Delta M = m(D^0 \gamma_c) - m(D^0)$

Fig. 6. Mass difference spectrum,  $\Delta M = m(D^0 \gamma_c) - m(D^0)$ .

$$R_{D_s^{*+}} \cdot \text{BR}(D_s^{*+} \rightarrow \phi \pi^+) = (5.3 \pm 1.3 \pm 1.2) \times 10^{-3}, \quad (6)$$

where  $R_{D_s^{*+}}$  is the production cross section relative to  $\sigma_{\mu\mu}$ , the muon pair production cross section. The two independent  $D_s^{*+}-D_s^+$  mass difference measurements are combined to give

$$\Delta M = 142.5 \pm 0.8 \pm 1.5 \text{ MeV}/c^2. \quad (7)$$

The mass of the  $D_s^+$  has been measured using the decay  $D_s^+ \rightarrow \phi \pi$  with the result

$$M_{D_s^+} = 1969.3 \pm 1.4 \pm 1.4 \text{ MeV}/c^2. \quad (8)$$

It is a pleasure to thank U. Djuanda, E. Konrad, E. Michel, and W. Reinsch for their competent technical help in running the experiment and processing the data. We thank Dr. H. Neemann, B. Sarau, and the DORIS group for the excellent operation of the storage ring. The visiting groups wish to thank the DESY directorate for the support and kind hospitality extended to them.

## References

- [1] M.K. Gaillard, B.W. Lee and J.L. Rosner, Rev. Mod. Phys. 47 (1975) 277.
- [2] ARGUS Collab., H. Albrecht et al., Phys. Lett. B 146 (1984) 111.
- [3] TPC Collab., H. Aihara et al., Phys. Rev. Lett. 53 (1984) 2465.
- [4] MARK III Collab., G. Blaylock et al., Phys. Rev. Lett. 58 (1987) 2171.
- [5] S. Godfrey and N. Isgur, Phys. Rev. D 32 (1985) 189; D.P. Stanley and D. Robson, Phys. Rev. D 21 (1980) 3180; M. Frank and P.J. O'Donnell, Phys. Lett. B 159 (1985) 174; K. Igi and S. Ono, Phys. Rev. D 32 (1985) 232.
- [6] ARGUS Collab., H. Albrecht et al., Phys. Lett. B 134 (1984) 137.
- [7] J. McKenna, Ph.D. Thesis (University of Toronto, 1987), unpublished.
- [8] ARGUS Collab., H. Albrecht et al., Phys. Lett. B 153 (1985) 343.
- [9] M. Suzuki, Phys. Lett. B 71 (1977) 139; C. Peterson et al., Phys. Rev. D 27 (1983) 105; B. Andersson et al., Phys. Rep. 97 (1983) 31.
- [10] P. Kim, Ph.D. Thesis (University of Toronto, 1987), unpublished.
- [11] Particle Data Group, M. Aguilar-Benitez et al., Review of particle properties, Phys. Lett. B 170 (1986) 1.
- [12] A. Drescher et al., Nucl. Instrum. Methods A 249 (1986) 277.